

Transport properties of $(\text{BiPb})_2\text{Sr}_2\text{Ca}_2\text{Cu}_3\text{O}_{10}$ textured tapes in the mixed state

M. R. Cimberle, C. Ferdeghini, D. Marré, M. Putti, and A. S. Siri

Consiglio Nazionale delle Ricerche, Istituto Nazionale per la Fisica della Materia, Dipartimento di Fisica, Via Dodecaneso 33, 16146 Genova, Italy

G. Grasso and R. Flükiger

Département de Physique de la Matière Condensée, 24 Quai Ernest-Ansermet, CH-1211 Genève 4, Switzerland

(Received 8 May 1995)

We discuss the resistivity, the Hall effect, the Nernst effect, and the magnetization in the mixed state taking the motion of the Abrikosov and Josephson vortices into account. Measurements on a $(\text{BiPb})_2\text{Sr}_2\text{Ca}_2\text{Cu}_3\text{O}_{10}$ tape point out how the contribution of the Josephson vortices to the resistivity ρ_J prevails at low temperatures and an analytical expression for ρ_J is proposed. Above the irreversibility line the Hall effect, the Nernst effect, and the magnetization are less affected by the granularity of the material and, at first approximation, can be considered to be intrinsic properties. Starting from this assumption, we calculate the contribution of the Abrikosov vortices to the resistivity ρ_A using the Nernst effect and the reversible magnetization data. The ρ_A thus calculated has an order of magnitude close to the values reported in literature for single crystals, and shows an activated behavior with temperature, whose activation energy value is in strict agreement with that measured in epitaxial thin films of $\text{Bi}(2223)$ compound.

I. INTRODUCTION

In the last years the study of the $(\text{BiPb})_2\text{Sr}_2\text{Ca}_2\text{Cu}_3\text{O}_{10}$ compound [$\text{Bi}(2223)$] has been arousing great interest. In fact, the weak link problem, which limits the performance of $\text{Y}(123)$, is less important in Bi cuprates; moreover, the $\text{Bi}(2223)$ has a higher transition temperature (110 K) than the $\text{Bi}(2212)$ phase, and appreciable values of pinning energies. These characteristics make $\text{Bi}(2223)$ the most promising candidate for practical applications. A fast technological development has led to the capability to realize long tapes carrying high critical currents (up to 42 kA/cm² at 77 K and zero field¹⁻³) using the "powder-in-tube" method; the samples so obtained are silver sheathed, with highly textured and strongly linked grains. The critical current depends strongly on the magnetic field and for further applicative development it is crucial to understand the dissipation mechanisms. In particular, great effort has been devoted to determine whether, in the presence of an applied magnetic field, the critical current is limited by intrinsic intragrain mechanisms or by intergrain dissipation. In order to understand the supercurrent behavior, phenomenological models related to the structure of the $\text{Bi}(2223)$ tapes have been proposed; they point out the role of the weak links between the platelike grains stacked like bricks in a wall⁴ or, alternatively, they assume that the small angle c -axis tilted grain boundaries constitute strong links.^{5,6} The field dependence analysis of the critical current indicates that at high temperatures the mechanism limiting the current arises from thermally activated flux creep of pancake vortices, while, as temperature and magnetic field decrease, granularity plays a dominant role.^{7,8} Till now, the electrical transport properties of the tapes have been

mainly characterized through analysis of the magnetization loops and current-voltage characteristics.⁶⁻¹⁶ In this paper, we present measurements of magnetoresistivity, Hall effect, Nernst effect, and reversible magnetization that allow us to investigate the dissipation mechanisms above the irreversibility line.

The galvanomagnetic and thermomagnetic effects in the mixed state arise from the motion of vortex lines due to an external driving force. Therefore, a close connection exists between the transport coefficients and a comparative analysis can help the comprehension of the various dissipative mechanisms present in a tape. In an isotropic superconductor the motion of the Abrikosov vortices plays a dominant role, but in high-temperature superconductors (HTSC's), various kinds of vortices must be considered. In fact, owing to the layered structure of these materials, when the magnetic field is applied perpendicular to the c axis, coreless vortices lie between the CuO_2 planes.¹⁷ Moreover, in a bidimensional system thermal fluctuations, as vortex antivortex pairs, can contribute to dissipation,¹⁸ but this contribution is negligible in the high field conditions we consider and, therefore, will be neglected in the following. On the contrary, in polycrystalline samples it is necessary to take into account the contribution of the Josephson vortices that are present in the links between the grain boundaries.

In the following sections we describe the magnetoresistivity, the Hall effect, the Nernst effect, and the magnetization in a polycrystalline sample, where the motion of the Abrikosov and Josephson vortices (between the CuO_2 planes and at the grain boundaries) must be taken into account. Measurements of the transport coefficients performed on $\text{Bi}(2223)$ textured tapes are analyzed and the different role played intergranular dissipation in the transport properties is discussed.

II. TRANSPORT PROPERTIES IN A POLYCRYSTALLINE SAMPLE

A. The contribution of the Abrikosov vortices

In the flux flow regime, in the presence of an applied current density \mathbf{J} , the Abrikosov vortices (V_A) move driven by the Lorentz force $\mathbf{F}_L = \mathbf{J} \wedge \phi_0$, where ϕ_0 is the flux quantum defined in the direction of the magnetic field; the Magnus force $\mathbf{F}_M = (\alpha/\phi_0)\mathbf{v}_\varphi \wedge \phi_0$ and the viscous force $\mathbf{F}_\eta = -\eta\mathbf{v}_\varphi$ arise because of the motion of vortex lines with velocity \mathbf{v}_φ , where α and η are Hall drag and the viscous coefficients, respectively. In the presence of pinning centers, Vinokur, Geshkenbein, and Feigel'man¹⁹ introduced a mean pinning force $\mathbf{F}_p = -\gamma\mathbf{v}_\varphi$ that opposes the vortex motion and renormalizes the viscous force. He finds a scaling law between ρ_{xy} and ρ_{xx} independent of disorder (α is not altered by pinning):

$$\rho_{xy} = \frac{\alpha}{\phi_0 B} \rho_{xx}^2, \quad (1)$$

This equation predicts a quadratic dependence between ρ_{xy} and ρ_{xx} observable in the low-temperature region where the small temperature dependence of α can be neglected with respect to the thermally activated behavior of ρ_{xx} . Experimental data for YBCO(123), Tl(2212), and Bi(2212) single crystals and epitaxial films^{20–24} confirm this theoretical approach and show a universal power law $\rho_{xy} = K\rho_{xx}^\beta$, with β ranging from 1.8 to 2 and K independent of the magnetic field; this implies that α scales linearly with the magnetic field. Equation (1) predicts that the Hall conductivity $\sigma_{xy} = \rho_{xy}(\rho_{xx}^2 + \rho_{xy}^2)^{-1} \approx \rho_{xx}/\rho_{xy}^2 \approx \alpha/\phi_0 B$ is independent of the disorder. This result was directly verified by Samoilov *et al.*²⁵

In the mixed state, when a thermal gradient ∇T is applied, both species carrying entropy, i.e., vortices and quasiparticles, diffuse driven by thermal forces. The occurrence of an electric field requires an active phase slip mechanism,²⁶ and therefore, transversal and longitudinal voltages appear owing to the motion of vortices only. The diffusion of normal quasiparticles, both bounded in the vortex core and unbounded outside it,^{27–29} contributes indirectly to dissipation causing a supercurrent counterflow that drives the vortices perpendicular to ∇T .^{30–32} This effect, not emphasized in conventional superconductors, gives rise to the Seebeck effect in the mixed state.

The Nernst voltage is generated by the diffusion of vortices under the effect of the thermal force $\mathbf{F}_{th} = -S_\varphi \nabla T$, where S_φ is the entropy of a flux line per unit length.³³ The viscous force balances the effect of \mathbf{F}_{th} and, according to the Josephson relation,²⁶ a voltage transversal to the temperature gradient appears. Neglecting the term proportional to the Hall angle, the Nernst effect is then given by:^{24,27,31,32}

$$QB \approx (S_\varphi/\phi_0)\rho_{xx}. \quad (2)$$

B. The contribution of the Josephson vortices

In HTSC's two kinds of Josephson vortices have to be taken into account: the Josephson vortices in the links at

the grain boundaries (V_{Jgb}) and the coreless vortices lying between the CuO_2 planes (V_{JCuO}). In order to estimate how the Josephson vortices contribute to the different transport coefficients, two aspects must be considered: (1) Coreless vortices cannot experience the same forces as vortices with a metallic core, and (2) in HTSC's the viscous coefficient is strongly anisotropic and the motion in certain directions can be inhibited.

In the presence of an applied current, the Lorentz force drives the Josephson and Abrikosov vortices alike. However, the V_{Jgb} , bounded along the grain boundaries, cannot move freely; therefore, the Magnus force, perpendicular to the vortex velocity, is counterbalanced by the bound reaction and the V_{Jgb} move contributing to the resistivity and not to the Hall effect.

In the case of the V_{JCuO} , owing to the layered structure of HTSC materials, the pinning force varies strongly with space. In particular, intrinsic pinning³⁴ opposes the motion in the c direction, while the V_{JCuO} move nearly free parallel to the ab planes. The problem of the vortex motion in a tilted magnetic field has been theoretically dealt with.³⁵ To evaluate qualitatively the V_{JCuO} contribution to the resistivity and to the Hall effect we have to consider two different situations: (1) \mathbf{J} parallel to the c axis: V_{JCuO} move freely parallel to the ab planes driven by the Lorentz force while the Magnus force is counterbalanced by the intrinsic pinning reaction (ρ_{xx} large and ρ_{xy} small). (2) \mathbf{J} perpendicular to the c axis: the Lorentz force is inhibited by intrinsic pinning, while the motion parallel to the ab planes is free, but, since \mathbf{v}_φ is small, the Magnus force is small (ρ_{xx} small and ρ_{xy} small).

In this simplified picture we have found that the V_{JCuO} contribution to the Hall effect is negligible, while V_{JCuO} contribute to the resistivity (mainly when $\mathbf{J} \parallel c$). Experimental data are in agreement with this analysis. ρ_{xy} was measured in a -axis- and in c -axis-oriented Eu-Ba-Cu-O thin films^{36,37} and it has been shown to be 50 times smaller when the field is applied perpendicular to the c axis. A similar result was obtained in a Bi(2223) melt textured sample, measured with $\mathbf{B} \parallel c$ and $\mathbf{B} \perp c$.³⁸ The Hall effect measured in a Y-Ba-Cu-O single crystal³⁹ in the configuration $\mathbf{J} \perp c$ is negligibly small below 84 K in a 10 T magnetic field, but shows large and negative values near the transition temperature. This is not in contrast with our analysis; in fact, at high temperatures the intrinsic pinning is less effective and, in the $\mathbf{J} \perp c$ configuration, the Magnus force is directed parallel to the ab planes where the friction coefficient is very low. In the presence of a thermal gradient, the thermal forces are related to the entropy carried by the vortices and, therefore, it was generally believed that the Josephson vortices contribute weakly to the thermomagnetic coefficients.^{40,41} In the case of the Seebeck effect this assumption was experimentally demonstrated by Samoilov, Yurgens, and Zavaritsky,³¹ who did not observe any magneto-Seebeck effect when the magnetic field was applied perpendicular to the c axis. Nevertheless, recently, Coffey emphasized the contribution of the moving Josephson vortices to the transport entropy.^{42,43} He calculated the entropy of moving vortices in low and intermediate field.⁴²

$$S_{\varphi} = -\frac{\phi_0}{4\pi} \frac{\partial H_{c1}}{\partial T}, \quad H_{c1} < H \leq 2H_{c1} \quad (3a)$$

$$S_{\varphi} = -\frac{\phi_0}{4\pi} \frac{\partial H_{c1}}{\partial T} \frac{\ln(H_{c2}/B)}{\ln k}, \quad 2H_{c1} < H \leq 2H_{c2} \quad (3b)$$

where H_{c1} and H_{c2} are the first and the second critical fields, respectively, and k is the Ginzburg-Landau parameter. In an anisotropic superconductor, the critical fields scale with the characteristic lengths as⁴⁴

$$H_{c1\parallel} = \frac{\phi_0}{4\pi\mu_0\lambda_{ab}^2} \ln k_{\parallel}, \quad H_{c1\perp} = \frac{\phi_0}{4\pi\mu_0\lambda_{ab}\lambda_c} \ln k_{\perp} \quad (4a)$$

$$H_{c2\parallel} = \frac{\phi_0}{2\pi\mu_0\xi_{ab}^2}, \quad H_{c2\perp} = \frac{\phi_0}{2\pi\mu_0\xi_{ab}\xi_c} \quad (4b)$$

where \parallel and \perp are relative to the c axis and λ_{ab} and λ_c are the penetration depths perpendicular and parallel to the c axis, and ξ_{ab} and ξ_c are the coherence lengths perpendicular and parallel to the c axis. Therefore, an approximate relation between the entropy of the coreless and the Abrikosov vortices can be obtained by using Eqs. (3) and (4):

$$S_{\varphi\perp} \approx \frac{\lambda_{ab}}{\lambda_c} S_{\varphi\parallel}. \quad (5)$$

The ratio $\Gamma = \lambda_c/\lambda_{ab}$ is the factor of anisotropy that in Y-Ba-Cu-O is of the order of 10 (Ref. 45) and in Bi-based compounds may be much larger;^{46,47} increasing the anisotropy $S_{\varphi\perp}$ becomes negligible in respect to $S_{\varphi\parallel}$ and the thermal force applied to the V_{JCuO} , too. The Nernst effect measurements in a Y-Ba-Cu-O melt textured sample⁴⁸ have been performed, varying the direction of magnetic field and thermal gradient in respect to the c axis. The authors analyzed the data using the relation (5) and emphasized the importance of anisotropy of the viscous coefficient. When $\mathbf{B}\perp c$ and $\nabla T\perp c$ the thermal force is small, but the resistive viscous force parallel to the ab planes is much smaller and a large Nernst voltage is observed; when $\mathbf{B}\perp c$ and $\nabla T\parallel c$ the intrinsic pinning is active and the Nernst effect is negligible.

It is not easy to estimate the V_{Jgb} contribution to the thermomagnetic effects. A measurement of the Nernst voltage in a Josephson junction of low-temperature superconductors has been reported,⁴⁹ but the experimental conditions ($H < H_{c1}$) were very different from those in which we are interested. On the one hand, if a proportionality between the entropy and the reversible magnetization exists [see below Eqs. (9) and (10)], we expect that at high field the entropy carried by vortices at the grain boundaries becomes negligible; on the other hand, our ignorance about the V_{Jgb} contribution to the thermomagnetic coefficients is increased by the fact that in a polycrystalline sample also the temperature gradient, to which V_{Jgb} are sensitive, is unknown. In conclusion, we do not know if the V_{Jgb} contribute to the Nernst effect in a significant way.

At this point, we summarize the results achieved so far. For the superposition principle, the electric fields arising from the motion of different kinds of vortices are additive. Therefore, in a polycrystalline sample, at high

fields and at temperatures far from the transition, we can write the resistivity, the Hall effect, and the Nernst effect as

$$\rho_{xx} \approx \rho_A + \rho_{\text{JCuO}} + \rho_{\text{Jgb}}, \quad (6)$$

$$\rho_{xy} \approx \rho_{\text{HA}}, \quad (7)$$

$$Q \approx Q_A + Q_{\text{JCuO}} + Q_{\text{Jgb}}(?), \quad (8)$$

where the subscripts A , JCuO , and Jgb indicate the contribution of V_A , V_{JCuO} , and V_{Jgb} , respectively; the question mark indicates that we are not able to estimate whether the Q_{Jgb} contribution is negligible or not.

Equations (6)–(8) have been written for an isotropic polycrystal, but in our case we deal with highly textured samples with $\mathbf{B}\parallel c$. In fact, these samples present a rocking angle of 8° determined by the full width at half maximum of rocking curves of the most intense (001) peaks of the x-ray diffraction pattern of the filament surface.⁵ A rocking angle of 8° implies that in an applied magnetic field the coreless vortices are one order of magnitude fewer than the pancake vortices. Moreover, the random orientation of the c axis implies a nearly equal number of coreless vortices and opposite vorticity; vortex and antivortex pairs contribute to the resistivity but not to the transversal voltages (Hall and Nernst effects).^{29,50,51} Therefore, in our case Eq. (8) may be simplified to

$$Q \approx Q_A + Q_{\text{Jgb}}(?). \quad (8')$$

III. THE MAGNETIZATION

A dc magnetization measurement integrates the magnetic response of the samples and it is not able to differentiate whether the magnetic signal originates from a connected region of the sample or not. Therefore, to separate the intragrain and intergrain contributions, the magnetization measurements should be supported by transport measurements. This kind of approach has pointed out that, in Bi(2223)-Ag tapes, in a region of high temperatures and high magnetic fields, the critical current flows on the same macroscopic scale both in magnetization and transport measurements.⁷ From magnetization and transport measurements, Cuthbert *et al.*⁷ deduced a phase diagram where the dominant dissipation regimes in the H - T plane are emphasized. Below the irreversibility line lies a region where the intragranular mechanisms are dominant (flux creep of the Abrikosov vortices); as temperature decrease the critical current of the grains increases exponentially and, when it reaches the critical current of the links between the grains, the limiting mechanism is related to the motion of the Josephson vortices. Therefore, in a low-temperature and low-field region, the dominant mechanism is the intergranular dissipation. This behavior is confirmed by transport measurements in Ref. 8.

At high fields the reversible magnetization of the Josephson junctions is negligible; therefore, in polycrystalline samples it is expected to be independent of the granularity of the materials, as confirmed by the diagram in Ref. 7. In highly anisotropic systems also the V_{JCuO} contribution to the reversible magnetization can be

neglected; in fact, the reversible magnetization is related to the first critical field H_{c1} through the London equation⁵² and, therefore, the strong anisotropy of H_{c1} [Eq. (4)] entails a strong anisotropy of the magnetization. In conclusion, the reversible magnetization is mainly due to the Abrikosov vortices.

In the reversible region a close correlation between the magnetization and the entropy carried by the vortices exists. Using the linearized microscopic theory near H_{c2} , Maki⁵³ obtained the result

$$S_{\varphi} = \frac{\phi_0}{T} L(T) M(T) = \frac{\phi_0}{T} L(T) \frac{H_{c2}(T) - H}{(2k^2 - 1)\beta_A}, \quad (9)$$

where $M(T)$ is the reversible magnetization and $L(T)$ is a function that is 1 near T_c and decreases monotonically as temperature decreases; in the last equality the reversible magnetization obtained by Abrikosov in the high-field limit has been included. Within the framework of the time-dependent Ginzburg-Landau theory, Troy and Dorsey⁵⁴ generalized this result to the entire mixed state; they found

$$U_{\varphi} = TS_{\varphi} = -\phi_0 M, \quad (10)$$

where U_{φ} is the thermal energy. Equations (9) and (10) coincide close to T_c . The validity of Eq. (10) has been well verified in Y-Ba-Cu-O compound, comparing dU_{φ}/dT obtained from the magnetization,⁵⁵ the Nernst effect,^{24,56} and the Ettingshausens effect.⁵⁷ Moreover, the U_{φ} curves, obtained from the Nernst effect measurements,²⁴ have been fitted using the model of Hao *et al.* for the reversible magnetization,⁵⁵ and the value found for the Ginzburg-Landau parameter k is in agreement with that obtained from magnetization measurement.⁵⁵

IV. EXPERIMENTAL DATA

All the experiments have been performed on Ag-sheathed Bi(2223) tapes. The samples were prepared by the powder in tube method, which is described in more detail elsewhere.^{6,58-60} Pure and reinforced Ag tubes were filled with precursor powders which were mainly composed of the Bi(2212) phase. The tubes were sealed and cold deformed by swaging and drawing to a final wire diameter of about 1 to 2 mm. In order to have a tapelike shape, the wires were rolled down to an overall thickness of about 100 μm . Finally, the tapes were treated at a temperature of about 830–840°C in order to form the Bi(2223) phase. The Bi(2223) grains are about 30 μm in diameter and they are highly textured (mean misalignment angle of about 8°). The critical current density of the tapes as enhanced by alternating heat treatments and densification steps, which are uniaxial pressing in the case of short samples and cold rolling in the case of long tapes. Typical J_c values at liquid nitrogen temperature and in the self-field of the tapes under investigation are generally above 20 kA/cm². The Bi(2223) filament normally accounts for about 30% of the total cross section. The Ag sheath was mechanically removed in order to avoid spurious effects on the transport properties.

The experimental apparatus for the transport measure-

ments, completely automated, allows one to perform a complete set of measurements in two temperature runs without changing the sample holder and contacts: in the first run, an electric current is applied and the magnetoresistivity and the Hall effect are measured; in the second, a thermal gradient is imposed and the Nernst and Seebeck effects are measured. In both cases, the magnetic field is increased up to 8 T and the direction is reversed to estimate the transversal voltages. The longitudinal and transversal voltages were measured with Cu wires with an accuracy of about 1 nV. The temperature differences were measured with a Au(0.7% Fe)-Chromel thermocouple using an ac technique: a 0.1–0.01 Hz alternating temperature difference, whose amplitude can be varied up to 100 mK, was applied to the sample; our sensitivity is less than 1 mK.

The magnetoresistivity, the Hall effect, and the Nernst effect are shown in Fig. 1 from 40 to 120 K in a magnetic field up to 8 T applied perpendicular to the tape plane. The resistivity just above the transition is of the order of

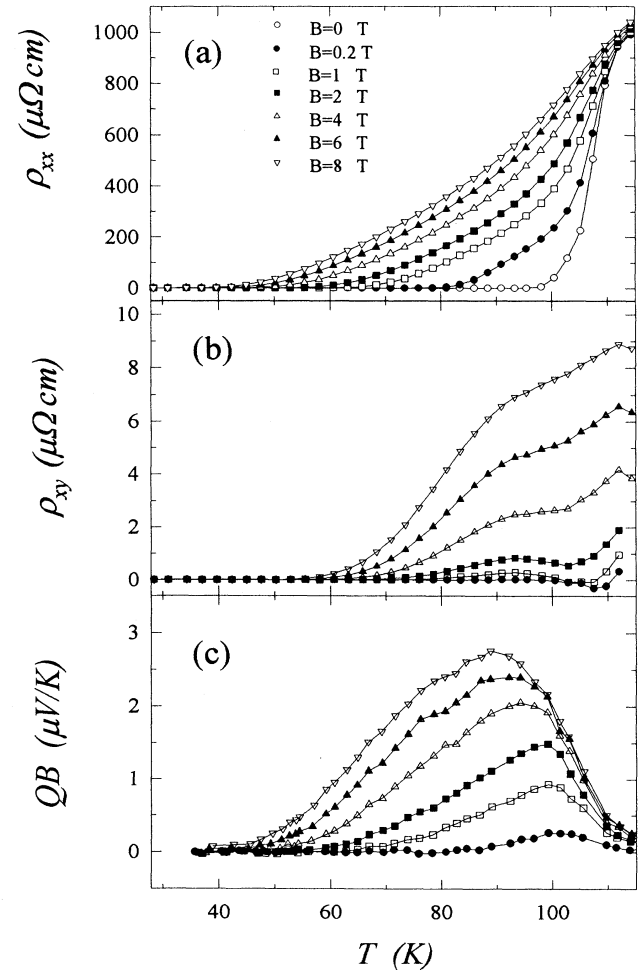


FIG. 1. (a) The resistivity, (b) the Hall effect, and (c) the Nernst effect from 40 to 120 K. The magnetic field was applied perpendicular to the tape.

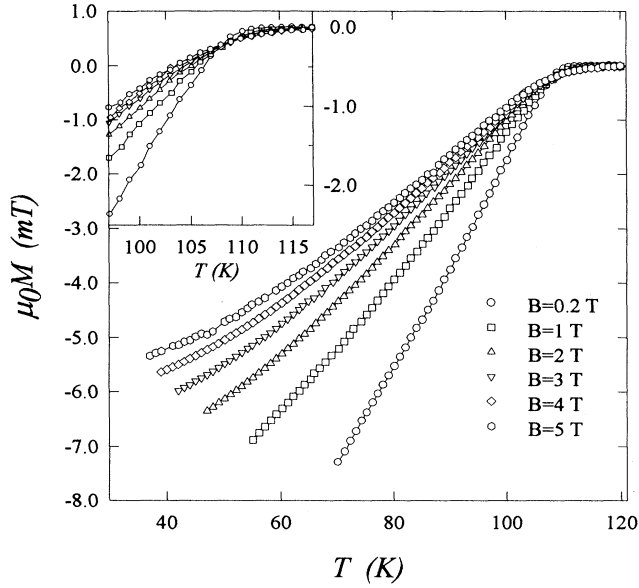


FIG. 2. Reversible magnetization versus temperature at $\mu_0 H = 0.2, 1, 2, 3, 4, 5$ T. In the inset an enlargement of the region near the transition is shown.

1 m Ω cm, a typical value for a polycrystal,⁶¹ then the curve steeply decreases showing a transition temperature onset of 110 K and a transition width of 7 K at zero field. Increasing the magnetic field the curves broaden and at 8 T the resistivity reaches zero at 40 K. Figure 1(b) shows the Hall effect. Starting from the normal state the Hall resistivity decreases, shows a minimum that for the lowest fields is negative, and then goes to zero. The change of sign of the Hall effect just below the transition temperature is common to all the HTSC materials and, despite numerous attempts to explain this anomaly, its origin remains unclear.^{39,62–66} The Nernst effect is reported in Fig. 1(c). In the normal state, QB is zero within our sensitivity;⁶⁷ 10 K above T_c it increases because of the thermal fluctuations,²⁴ passes through a maximum, which is 100 K at 0.2 T, and shifts to 90 K at 8 T, then vanishes to zero.

The dc magnetization was measured in a Quantum Design superconducting quantum interference device magnetometer in a field up to 5.5 T, in a temperature range from 5 to 150 K; the magnetic moment was measured with an accuracy of 10^{-9} A m². The magnetic field was applied parallel to the c axis of the sample and the magnetization was measured above the irreversibility line¹⁵ detected by a deformation of the magnetic response when the sample is moved through the coils.⁶⁸ Figure 2 shows the magnetization in the reversible region. A temperature-independent diamagnetic susceptibility, measured in the normal state, has been subtracted. The figure inset shows an enlargement of the transition region. A rounding of the $M(T, H)$ curves becomes remarkable as the field increases, indicating an enhancement of the fluctuation contribution.^{69–71} One of the characteristic features is the existence of a crossing point

at which the magnetization takes a constant value independent of the magnetic field.⁷¹ Our experimental result yields the value of $\mu_0 M^* = -0.26$ mT at the crossing point $T^* = 108.5$ K, in agreement with Ref. 72.

V. DISCUSSION

A. The magnetoresistivity, the Hall effect, and the Nernst effect

We start by considering the scaling relation between the magnetoresistivity and the Hall resistivity; in Fig. 3 we plot ρ_{xy} versus ρ_{xx} in a log-log scale. The straight line in the plot corresponds to $\rho_{xy} \propto \rho_{xx}^\beta$ with $\beta = 2.9$. Actually, the experimental data, best fitted in the low-temperature region only, follow a power law with $\beta = 2.2, 2.8, 3,$ and 3.2 at $\mu_0 H = 1, 4, 6,$ and 8 T, respectively. Therefore, as the field increases, our data depart from the Vinokur relation ($\beta = 2$), and, as for other polycrystalline samples,⁷³ show a scaling law with $\beta \approx 3$. Let us show what $\beta > 2$ entails. From Eqs. (6) and (7) it follows that the measured Hall resistivity is given by $\rho_{xy} \approx \rho_{\text{HA}}$, while $\rho_{xx} \approx \rho_A + \rho_J$, where ρ_J indicates both the Josephson contributions to the resistivity. Therefore, in the low-temperature region, we can write

$$\rho_{xy} \approx \rho_{\text{HA}} \propto (\rho_A + \rho_J)^\beta, \quad (11)$$

where $\beta > 2$. For a single crystal inside our sample, in a magnetic field $\mathbf{B} \parallel c$, it must be $\rho_{xy} = \rho_{\text{HA}}$, and $\rho_{xx} = \rho_A$ related by the scaling law

$$\rho_{xy} = \rho_{\text{HA}} \propto \rho_A^2. \quad (12)$$

Equalizing Eqs. (11) and (12) we find

$$1 + \frac{\rho_J}{\rho_A} \propto \rho_A^{-(\beta-2)/\beta}. \quad (13)$$

Equation (13) means that, for β going to 2, the right

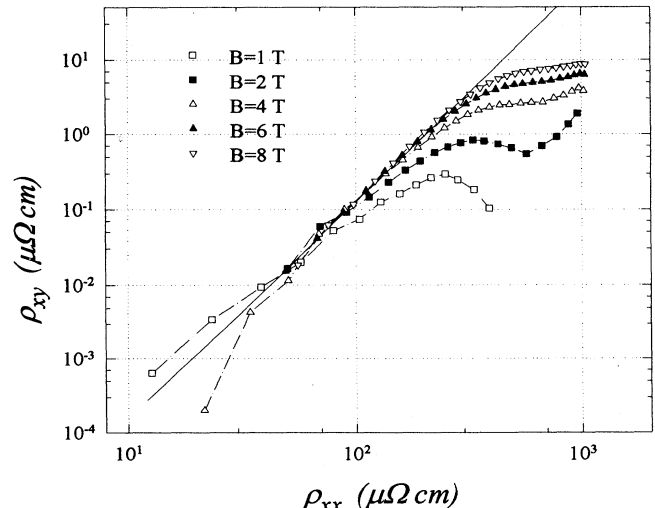
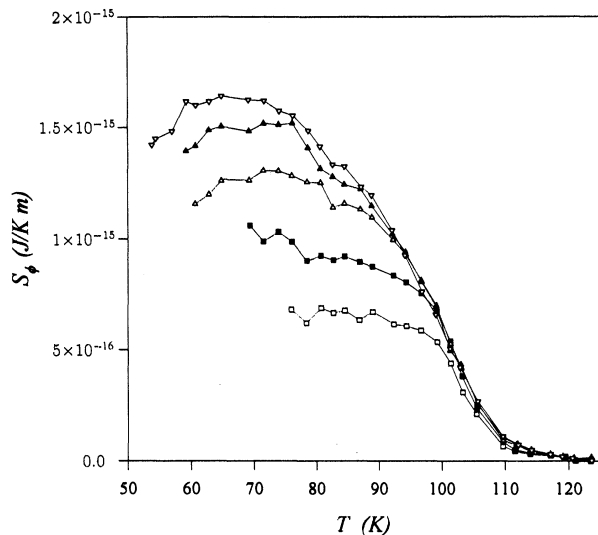


FIG. 3. ρ_{xy} versus ρ_{xx} in a log-log plot; the straight line corresponds to $\rho_{xy} \propto \rho_{xx}^\beta$ with $\beta = 2.9$.

FIG. 4. $QB\phi_0/\rho_{xx}$ versus temperature.

member is independent of ρ_A and equal to 1, and ρ_J vanishes; as β increases, the right member depends more and more on ρ_A and the strong temperature dependence of ρ_A entails that the ratio ρ_J/ρ_A diverges at low temperatures where ρ_A goes to zero. Thus, we find that, at a fixed field (i.e., fixed β), the contribution of the Josephson vortices to the resistivity predominates in the low-temperature region while, as temperature increases, it becomes less important; this confirms that the long tail in the magnetoresistivity of polycrystalline samples may be attributed to the weak link dissipation. The field dependence of the ratio ρ_J/ρ_A is less clear. We find that β decreases with decreasing field, and the ratio ρ_J/ρ_A too; but, decreasing the field, ρ_A vanishes at higher temperature. Therefore, varying the field, the temperature ranges where Eq. (13) is valid are different, and the ranges do not overlap. In conclusion, one of our results is that, in agreement with other experimental evidences,^{11,12} the intergrain dissipation predominates at low temperature. The relation (13) may be checked by comparison with the thermomagnetic effect. We consider the relation between the Nernst effect and the resistivity. In Fig. 4, we plot $QB\phi_0/\rho$ which for the Abrikosov vortices [Eq. (2)], is equal to the entropy S_φ . We find a family of curves that rises from zero near T_c and then reaches a nearly constant value that, as the field increases, is higher. As we discussed in Sec. III, the transported entropy is proportional to the magnetization and, therefore, it is expected to have a field dependence opposite to the one we find. Behaviors such as those presented in Fig. 4 were often observed in polycrystalline samples,^{40,61} while recently, S_φ measurements showed the right relation with the magnetization.²⁴ As proposed in Ref. 74, we seek the explanation of this opposite field dependence in the contribution of the Josephson vortices to the resistivity. Using Eqs. (6) and (8') where, at first approximation, we make the further hypothesis $Q \approx Q_A$, we can write

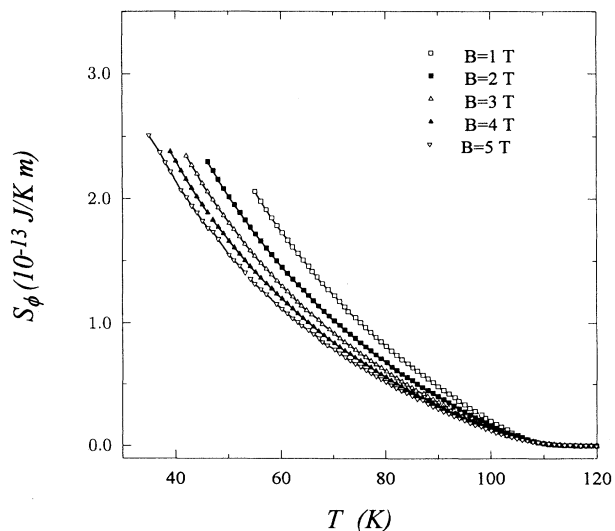
$$\frac{QB\phi_0}{\rho} \approx \frac{Q_A B\phi_0}{(\rho_A + \rho_J)} \approx \frac{Q_A B\phi_0}{\rho_A} \frac{1}{1 + \rho_J/\rho_A} \propto S_\varphi \rho_A^{-(\beta-2)/\beta}, \quad (14)$$

where in the last equality we used Eqs. (2) and (13). ρ_A increases strongly with the field, while S_φ , proportional to the magnetization, slowly decreases with the field; therefore, Eq. (14) increases with the field and thus we can explain the field dependence shown in Fig. 4. Practically it is not necessary to invoke some spurious contribution to the measured Nernst effect to explain the experimental results and, even though we cannot exclude some further terms in Q [see Eq. (8')], we can consider them to be not remarkable.

B. The Abrikosov contribution to the resistivity

In the section above we have evaluated that in our sample the contribution of the Josephson vortices to the resistivity prevails at least in the low-temperature region, while the main contribution to the Nernst effect seems to be given by the motion of the Abrikosov vortices. Starting from these assumptions, we try to estimate the Abrikosov contribution to the resistivity.

We consider the magnetization curves in Fig. 2, and recalling (see Sec. III) that it is well verified that the reversible magnetization is due to the Abrikosov vortices only, from Eq. (10) we calculate the entropy as $S_\varphi = \phi_0 M/T$. S_φ is reported in Fig. 5 for $\mu_0 H = 1, 2, 3, 4, 5$ T. We can observe that the behavior of these curves is different from what we found in Fig. 4; the field dependence is opposite and the absolute value is one order of magnitude higher. We have seen that the anomalies of the curves in Fig. 4 can be explained assuming that only the magnetoresistivity is affected by weak link dissipation, while the Nernst effect may be considered to be an intrinsic effect. Follow-

FIG. 5. S_φ for the Abrikosov vortices as calculated from Eq. (10).

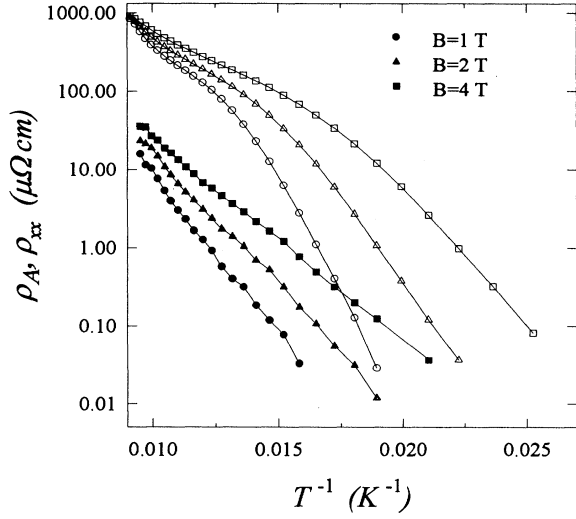


FIG. 6. ρ_{xx} (open symbols) and ρ_A (solid symbols) versus temperature as a function of $1/T$, at $\mu_0 H = 1, 2,$ and 4 T.

ing the same framework, we can calculate the contribution to the resistivity due to the motion of the Abrikosov vortices as

$$\rho_A \approx \frac{QB\phi_0}{S_\varphi} \approx \frac{QBT}{M}. \quad (15)$$

In Fig. 6 we show in an Arrhenius plot the resistivity curves so obtained at 1, 2, and 4 T; for comparison the magnetoresistivity ρ_{xx} measured at the same fields has been reported. We can observe that ρ_A has a value, a temperature behavior, and a field dependence in good agreement with the magnetoresistivity of Y-Ba-Cu-O and Bi(2212) single crystals.^{57,63,75,76} Because of the numerous approximations made and of the unusual procedure used to evaluate ρ_A , this result may appear astonishing. At temperatures near the transition (the calculation has been stopped at 105 K), the curves do not join together, maybe because some dissipation mechanisms (such as quasiparticles, fluctuation, etc.) were not considered in our calculation. In the whole temperature range ρ_A shows an activated behavior. We have calculated the activation energy U_0 by fitting the data with an exponential law; the U_0 values so obtained are 950, 760, and 600 K at 1, 2, and 4 T, respectively, and are in strict agreement with those found on Bi(2223) epitaxial films oriented with $\mathbf{B} \parallel \mathbf{c}$.⁴⁷

Comparing ρ_A with ρ_{xx} , we find that the calculated curves are more than one order of magnitude lower than the measured ones. At first sight this difference might seem excessive, but reflects exactly the difference between the transition resistivity of a polycrystal (1–1.5 m Ω cm) and that of a single crystal (50–100 $\mu\Omega$). So we have found that, at first approximation the measured ρ_{xx} represents only the Josephson contribution ρ_J . This allows us to check the validity of Eq. (13) which predicts an increasing ratio ρ_J/ρ_A with decreasing temperature. This behavior is confirmed looking over Fig. 6; in fact, we

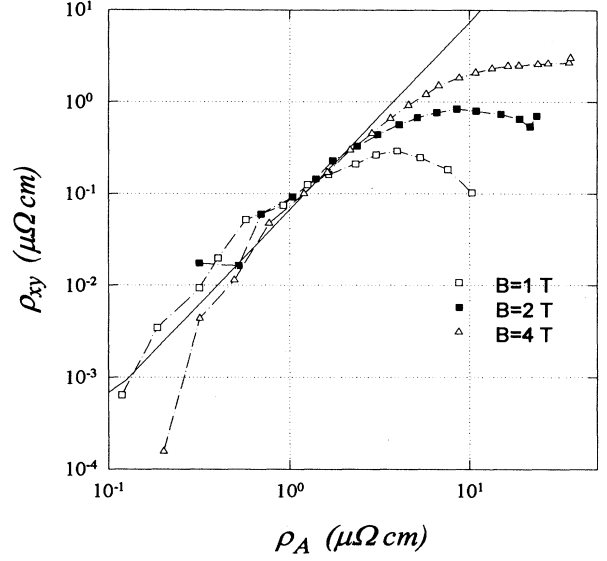


FIG. 7. ρ_{xy} versus ρ_A in a log-log plot; the straight line corresponds to $\rho_{xy} \propto \rho_A^\beta$ with $\beta=2$.

find that at all fields the ratio ρ_J/ρ_A is about 30 at the highest temperatures and becomes 100 at the lowest temperatures at which ρ_A has been estimated. For further decrease of temperature the slope of ρ_{xx} increases, but we are not able to calculate ρ_A because we enter the irreversibility region.

These results encourage us to think that the ρ_A evaluation might be correct. As a further check, we present the scaling law between the measured ρ_{xy} and ρ_A . In Fig. 7, we report ρ_{xy} versus ρ_A in a log-log plot for $\mu_0 H = 1, 2,$ and 4 T; the solid line represents $\rho_{xy} \propto \rho_A^\beta$ with $\beta=2$. We see that, even though the data are a little noisy, in the low-temperature region they are in good agreement with the model of Vinokur, Geshkenbein, and Feigel'man,¹⁹ while we recall that the scaling law between ρ_{xy} and ρ_{xx} at 4 T gives $\beta=2.8$.

This last result confirms our starting point which assumed that the Hall resistivity is mainly due to the motion of Abrikosov vortices. Moreover, since ρ_A has been calculated from the Nernst effect and the magnetization [see Eq. (16)], our conclusion is that to the Josephson vortices play an unimportant role in such properties. This conclusion appears even more remarkable considering that the magnetoresistivity is dominated by weak link dissipation.

VI. CONCLUSION

In this paper we have made a comparative analysis of the transport coefficients in a Bi(2223) tape in order to point out the contribution of the Josephson vortices to dissipation. Starting from the assumption that the Hall resistivity is not affected by weak link contributions, we have obtained for the ratio ρ_J/ρ_A a relation indicating that the contribution of the Josephson vortices to the resistivity prevails in the low-temperature region. This

result goes in the direction outlined by magnetization and critical current measurements, where a dominant weak link dissipation is observed at low temperatures and low fields.^{7,8} Nevertheless, the Hall and Nernst effects do not seem to be so affected by the weak link dissipation as we have inferred in the following ways. First, we have analyzed the ρ - Q scaling relation: considering the ρ_J contribution only, we explained the observed anomalies without the necessity to invoke a considerable weak link contribution to Q . Second, we have analyzed the reversible magnetization. M provides an independent estimate of the entropy S_φ that, together with the Nernst effect, has allowed us to evaluate the resistivity of the Abrikosov vortices ρ_A . The ρ_A so calculated shows an order of magnitude, a temperature behavior, and a field dependence very close to those observed in HTSC single crystals and the activation energies calculated by the Arrhenius plot are in good agreement with the values obtained in Bi(2223) epitaxial thin films. Finally, the scaling relation between the measured ρ_{xy} and the calculated ρ_A is in very good agreement with the Vinokur law.

The comparative analysis of different measurements and the overall consistency of the results lead us to conclude that in our Bi(2223) tape, analyzed in the reversible region, intragrain and intergrain mechanisms play different roles in the transport properties; in particular,

the magnetoresistivity is dominated by weak link dissipation, while the Hall and the Nernst effects are weakly perturbed by the granularity of the material.

Our results are clearly related to the characteristics of the samples considered, but give a contribution to the comprehension of important issues. In particular, to understand the cause of the resistivity transition broadening in an applied magnetic field is strictly related to the technological approaches that study the enhancement of the critical current. More fundamental information has come from the other transport properties. Hall resistivity measurements in Josephson junctions and in B1c configuration can help to clarify the real meaning of the Magnus force and a controversial phenomenon such as the sign reversal of the Hall effect in the mixed state. How the Josephson vortices contribute to the thermomagnetic effects is another open issue related both to the effective entropy carried by coreless vortices and to the anisotropy of the viscous force; also in this case more direct measurements on well-characterized samples are necessary.

ACKNOWLEDGMENTS

This work was partially supported by INFN, CNR, and the BRITE EURAM Contract No. BRE2-0229.

-
- ¹K. Sato, K. Ohkura, K. Hayashi, M. Ueyama, J. Fujikami, and T. Kato, *Physica B* (to be published).
- ²G. Grasso, A. Jeremie, B. Hensel, and R. Flükiger, *IEEE Trans. Appl. Supercond.* **5**, 1255 (1995).
- ³G. N. Riley, Jr., *Physica C* **235-240**, 3407 (1994).
- ⁴L. N. Bulaevskii, J. R. Clem, L. I. Glazman, and A. P. Malozemoff, *Phys. Rev. B* **45**, 2545 (1992).
- ⁵B. Hensel, J. C. Grivel, A. Jeremie, A. Perin, A. Pollini, and R. Flükiger, *Physica C* **205**, 329 (1993).
- ⁶B. Hensel, G. Grasso, and R. Flükiger, *Phys. Rev. B* **51**, 15 456 (1995).
- ⁷M. N. Cuthbert, M. Dhalle, G. K. Perkins, L. F. Cohen, Y. C. Guo, H. K. Lu, G. Grasso, R. Flükiger, S. Penn, T. Beales, and A. D. Caplin, *Physica C* **235-240**, 3027 (1994).
- ⁸G. Fuchs, A. Gladun, K. Fischer, T. Staiger, and P. Verges, *Physica C* **235-240**, 3101 (1994).
- ⁹G. Ries, H. W. Neumuller, W. Schmidt, and C. Struller, in *Proceedings of the 7th International Workshop on Critical Current in Superconductors, 24 Jan 1994, Alpbach, Austria*, edited by H. W. Weber (World Scientific, Singapore, 1994).
- ¹⁰S. P. Ashworth and B. A. Glowacki, *Physica C* **26**, 159 (1994).
- ¹¹A. D. Caplin, S. M. Cassidy, L. F. Cohen, M. N. Cuthbert, J. R. Lavery, G. K. Perkins, S. X. Dou, Y. C. Guo, H. K. Lu, H. J. Tao, and E. L. Wolf, *Physica C* **209**, 167 (1993).
- ¹²M. Dämpling, G. Grasso, and R. Flükiger, *Physica C* **235-240**, 3029 (1994).
- ¹³M. Suenaga, Q. Li, Y. Fukumoto, K. Shibusaki, Y. L. Wang, H. J. Wiesmann, P. Haldar, and L. Motowidlo, in *Critical State in Superconductors*, Proceedings of the 1994 Topical International Cryogenic Materials Conference, Honolulu, 1994, edited by K. Tachikawa, K. Kitazawa, H. Maeola, and T. Matsushita (World Scientific, Singapore, 1995).
- ¹⁴T. Hikata, M. Ueyama, H. Mukai, and K. Sato, *Cryogenics* **30**, 924 (1990).
- ¹⁵V. Calzona, M. R. Cimberle, C. Ferdeghini, R. Flükiger, G. Grasso, M. Putti, C. Rizzuto, and A. S. Siri, *Cryogenics ICEC Suppl.* **34**, 801 (1994).
- ¹⁶V. Calzona, M. R. Cimberle, C. Ferdeghini, R. Flükiger, E. Giannini, G. Grasso, D. Marré, M. Putti, and A. S. Siri, *Physica C* (to be published).
- ¹⁷J. R. Clem and M. W. Coffey, *Phys. Rev. B* **42**, 6209 (1990); J. R. Clem, *ibid.* **43**, 7837 (1991).
- ¹⁸J. M. Kosterlitz and D. J. Thouless, *J. Phys. C* **6**, 1181 (1973).
- ¹⁹V. M. Vinokur, V. B. Geshkenbein, and M. V. Feigel'man, *Phys. Rev. Lett.* **71**, 1242 (1993).
- ²⁰A. V. Samoilov, *Phys. Rev. Lett.* **71**, 617 (1993).
- ²¹R. C. Budhani, S. H. Liu, Z. X. Cai, and Z. Wang, *Phys. Rev. Lett.* **71**, 621 (1993).
- ²²P. J. M. Woeltgens, C. Dekker, and H. W. de Wign, *Phys. Rev. Lett.* **71**, 3858 (1993).
- ²³A. V. Samoilov, Z. G. Ivanov, and L. G. Johansson, *Phys. Rev. B* **49**, 3667 (1994).
- ²⁴H.-C. Ri, R. Gross, F. Gollnik, A. Beck, R. P. Huebener, P. Wagner, and H. Adrian, *Phys. Rev. B* **50**, 3312 (1994).
- ²⁵A. V. Samoilov, A. Legris, F. Rullier-Albenque, P. Lejay, S. Buffard, Z. G. Ivanov, and L. G. Johansson, *Physica C* **235-240**, 3141 (1994).
- ²⁶B. D. Josephson, *Phys. Lett.* **16**, 242 (1965).
- ²⁷E. Z. Meilikhov and R. M. Farzetdinova, *Physica C* **221**, 27 (1994).
- ²⁸V. Calzona, M. R. Cimberle, C. Ferdeghini, D. Marré, M. Putti, A. S. Siri, G. Grasso, and R. Flükiger, *Physica C*

- 235-240, 3113 (1994).
- ²⁹V. Calzona, M. R. Cimberle, C. Ferdeghini, D. Marré, and M. Putti, *Physica C* **246**, 169 (1995).
- ³⁰R. P. Huebener, A. V. Ustinov, and V. K. Kapulenko, *Phys. Rev. B* **42**, 4831 (1990).
- ³¹A. V. Samoilov, A. A. Yurgens, and N. V. Zavaritsky, *Phys. Rev. B* **46**, 6643 (1992).
- ³²H.-C. Ri, F. Kober, A. Beck, L. Alff, R. Gross, and R. P. Huebener, *Phys. Rev. B* **47**, 12 312 (1993).
- ³³R. P. Huebener, in *Magnetic Flux Structures in Superconductors*, edited by M. Cardona *et al.*, Vol. b of Springer Series in Solid-State Sciences (Springer, Berlin, 1979).
- ³⁴M. Tachiki and S. Takahashi, *Solid State Commun.* **70**, 291 (1989).
- ³⁵E. Z. Meilikhov and R. M. Farzetdinova (unpublished).
- ³⁶J. Colino, M. A. Gonzalez, J. I. Martin, M. Velez, D. Oyola, P. Prieto, and J. L. Vicent, *Phys. Rev. B* **49**, 3496 (1994).
- ³⁷J. I. Martin, M. Velez, J. Colino, M. A. Gonzalez, and J. L. Vincent, *Physica C* **235-240**, 3123 (1994).
- ³⁸P. Vasek, I. Janacek, and V. Plechacek, *Physica C* **235-240**, 3145 (1994).
- ³⁹J. M. Harris, N. P. Ong, and Y. F. Yan, *Phys. Rev. Lett.* **71**, 1455 (1993).
- ⁴⁰F. Kober, H.-C. Ri, R. Gross, D. Koelle, R. P. Huebener, and A. Gupta, *Phys. Rev. B* **44**, 11 951 (1991).
- ⁴¹R. P. Huebener *et al.*, *Physica C* **181**, 345 (1991).
- ⁴²M. W. Coffey, *Phys. Rev. B* **48**, 9767 (1993).
- ⁴³M. W. Coffey, *Physica C* **233**, 409 (1994).
- ⁴⁴D. Feinberg, *J. Phys. III (France)* **4**, 169 (1994).
- ⁴⁵Y. Iye *et al.*, *Physica C* **153-155**, 26 (1988); U. Welp *et al.*, *Phys. Rev. Lett.* **62**, 1908 (1989); W. Bauhofer *et al.*, *ibid.* **63**, 2520 (1989).
- ⁴⁶D. E. Farrell, S. Bonham, J. Foster, Y. C. Chang, P. Z. Jang, K. G. Vandervoort, D. J. Lam, and V. G. Kogan, *Phys. Rev. Lett.* **63**, 782 (1989).
- ⁴⁷I. Matsubara, H. Tanigawa, T. Ogura, H. Yamashita, and M. Kinoshita, *Phys. Rev. B* **45**, 7414 (1992).
- ⁴⁸T. Sasaki, J. Ikeda, N. Kobayashi, K. Watanabe, M. Sawamura, K. Kimura, K. Miyamoto, and M. Hashimoto, *Physica C* **235-240**, 3175 (1994).
- ⁴⁹G. Y. Logvenov, V. A. Larkin, and V. V. Ryazanov, *Phys. Rev. B* **48**, 16 853 (1992).
- ⁵⁰Y. Matsuda, S. Komiyama, T. Terashima, K. Shimura, and Y. Bando, *Phys. Rev. Lett.* **69**, 3228 (1992).
- ⁵¹R. Gross, H.-C. Ri, F. Gollnik, and R. P. Huebener, *Physica B* **194-196**, 1365 (1994).
- ⁵²M. Tinkham, *Introduction to Superconductivity* (McGraw-Hill, Tokyo, 1975), p. 154.
- ⁵³K. Maki, *J. Low Temp. Phys.* **1**, 45 (1969).
- ⁵⁴R. J. Troy and A. T. Dorsey, *Phys. Rev. B* **47**, 2715 (1993).
- ⁵⁵Z. Hao, J. R. Clem, M. W. McElfresh, L. Civale, A. P. Malozemoff, and F. Holtzberg, *Phys. Rev. B* **43**, 2844 (1991).
- ⁵⁶S. J. Hagen, C. J. Lobb, R. L. Greene, M. G. Forrester, and J. Talvacchio, *Phys. Rev. B* **42**, 6777 (1990); **43**, 6247 (1991).
- ⁵⁷T. T. M. Palstra, B. Batlogg, L. F. Schneemeyer, and J. V. Waszczak, *Phys. Rev. Lett.* **64**, 3090 (1990).
- ⁵⁸G. Grasso, A. Perin, B. Hansel, and R. Flükiger, *Physica C* **217**, 335 (1993).
- ⁵⁹Y. Yamada, B. Oobst, and R. Flukiger, *Supercond. Sci. Technol.* **4**, 165 (1991).
- ⁶⁰R. Flukiger, B. Hansel, A. Jeremie, M. Decroux, H. Kupfer, E. Seibt, W. Goldacker, and Y. Yamada, *Supercond. Sci. Technol.* **5**, S61 (1992).
- ⁶¹A. Dascolidou, M. Galfy, C. Hohn, N. Knauf, and A. Freimuth, *Physica C* **210**, 202 (1992).
- ⁶²Y. Iye, S. Nakamura, and T. Tamegai, *Physica C* **159**, 616 (1989).
- ⁶³T. R. Chien, T. W. Jing, N. P. Ong, and Z. Z. Wang, *Phys. Rev. Lett.* **66**, 3075 (1991).
- ⁶⁴S. J. Hagen, C. J. Lobb, R. L. Greene, and J. H. Kang, *Phys. Rev. B* **41**, 11 630 (1990); **43**, 6246 (1991).
- ⁶⁵J. P. Rice, N. Rigakis, D. M. Ginsberg, and J. M. Mochel, *Phys. Rev. B* **46**, 11 050 (1992).
- ⁶⁶M. V. Feigel'man, V. B. Geshkenbein, A. I. Larkin, and V. M. Vinokur, *Physica C* **235-240**, 3127 (1994).
- ⁶⁷J. A. Cayhold, A. W. Linnen, Jr., F. Chen, and C. W. Chu, *Physica C* **235-240**, 1537 (1994).
- ⁶⁸M. Suenaga, D. O. Welch, and R. Budhani, *Proceedings of the 6th International Workshop on Critical Currents [Supercond. Sci. Technol. S1* (1991)].
- ⁶⁹S. Ullah *et al.*, *Phys. Rev. Lett.* **65**, 2066 (1990); *Phys. Rev. B* **44**, 262 (1991).
- ⁷⁰R. Ikeda *et al.*, *Phys. Rev. Lett.* **67**, 3874 (1992); *J. Phys. Soc. Jpn.* **60**, 1051 (1991).
- ⁷¹Z. Tesanovic, L. Xing, L. Bulaevskii, Q. Li, and M. Suenaga, *Phys. Rev. Lett.* **69**, 3563 (1992).
- ⁷²N. Kobayashi, K. Egawa, K. Miyoshi, H. Iwaasaki, H. Ikeda, and R. Yoshizaki, *Physica C* **219**, 265 (1994).
- ⁷³M. Viret and J. M. D. Coey, *Phys. Rev. B* **49**, 3475 (1994).
- ⁷⁴V. Calzona, M. R. Cimberle, C. Ferdeghini, D. Marré, M. Putti, A. S. Siri, and G. Grasso, *Nuovo Cimento D* **16**, 1827 (1994).
- ⁷⁵T. T. Palstra, B. Batlogg, L. F. Schneemeyer, and J. V. Waszczak, *Phys. Rev. Lett.* **61**, 1662 (1988).
- ⁷⁶T. T. M. Palstra, B. Batlogg, R. B. van Dover, L. F. Schneemeyer, and J. V. Waszczak, *Phys. Rev. B* **41**, 6621 (1990).